Electronic Supplementary Information (ESI) for ChemComm

A General Synthetic Method towards Conjugated Microporous Polymers with Ordered Bicontinuous Mesostructures

Qiqi Yang, Yamei Liu, Luoxing Xiang, Jiacheng Zhang, Yucheng Yin, Fugui Xu, and Yiyong Mai*

School of Chemistry and Chemical Engineering, Frontiers Science Center for Transformative Molecules, Shanghai Key Laboratory of Electrical Insulation and Thermal Ageing, Shanghai Jiao Tong University, 800 Dongchuan Road, Shanghai 200240, China

E-mail: mai@sjtu.edu.cn

Table of Contents

1. Experimental section

1.1 Materials

Monomethoxy poly(ethylene oxide) (monomethoxy-PEO2000), CuBr, styrene, 2-bromoisobutyryl, triethylamine, *N,N,N',N',N''*-pentamethyldiethylenetriamine (PMDETA), tetrahydrofuran, tetraethyl orthosilicate (TEOS), hexaketocyclohexane octahydrate, 1,2,4,5-tetraaminobenzene tetrahydrochloride, 3,3',4,4'-tetraaminobiphenyl and 2,3,5,6-Tetraaminobenzoquinone were purchased from Sigma-Aldrich and used as received, unless otherwise mentioned.

1.2 Synthesis of PS-*b*-PEO

The PS-*b*-PEO block copolymer was synthesized *via* atom transfer radical polymerization (ATRP) method involving two steps (Figure S1).[1] In the first step, monomethoxy PEO2000 (50 g, 0.025 mol) was dissolved in dichloromethane (DCM, 200 mL) under stirring in a dried Schlenk-flask. Afterwards, triethylamine (10.1 mL, 7.5 mmol) was added in and the mixture was cooled down to 0 °C, followed by the dropping of bromoisobutyryl bromide (6.2 mL, 0.05 mol) into the flask. After stirring for 12 hours in an ice-water bath, triethylamine salt was removed by filtration. The residue solution was concentrated to *ca*. 50 mL by rotary evaporation, and subsequently precipitated into cold ether under vigorous stirring. The obtained suspension was then stored at 0 °C for 24 hours, and the white precipitate was filtered and washed with cold ether for three times. Finally, the white product was obtained after being dried under vacuum at room temperature overnight. In the second step, 2 g PEO_{45}-Br (0.84 mmol), 133 mg CuBr (0.93 mmol) and 206 μL PMDETA (1 mmol) were added in a flame-dried

Schlenk-flask, followed by the operation of vacuumizing and refilling with N_2 for three cycles, to thoroughly remove O_2 in the container. Afterwards, a calculated amount of styrene was injected into the flask via a syringe, and the mixture was deoxygenated by freeze-pump-thaw for three cycles. Subsequently, the flask was immersed in an oil bath with a heating temperature of 110 °C under stirring. One night later, the polymerization was terminated by removal of the heat source and subsequently cooling by liquid nitrogen. Subsequently, the product was dissolved in THF and passed through a short column of basic alumina to remove copper complexes. The solution was concentrated and precipitated into a large excess of methanol. The white floccule was then filtered and washed with methanol for three times, and finally dried under vacuum for 24 hours.
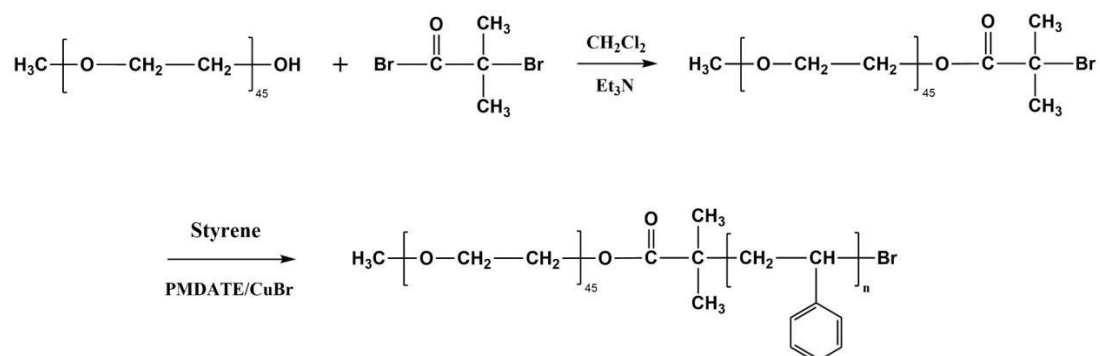

Figure S1. The synthetic route towards PS-*b*-PEO.

1.3 Synthesis of SDD-SiO$_2$

SiO$_2$ with SDD structures was prepared by the solvent evaporation-induced self-assembly (EISA) method.[2] First, PS$_{252}$-*b*-PEO$_{45}$ (75 mg) was dissolved in THF (5 mL) under stirring at room temperature for 30 min, followed by adding HCl solution (2M, 500 μL) to the solution. After an hour of stirring, TEOS (320 μL) was added to the mixture, and the solution was then moved to a desiccator for the process of evaporation. 3 days later, self-assembly was completed and the mixture was subsequently transferred

to the oven and maintained under a heating temperature of 100 °C for additional 24 hours. Finally, the as-prepared samples were calcined at 550 °C in air for 8 h.

1.4 Preparation of SDD-Aza-CMP-1

Hexaketocyclohexane octahydrate (18.7 mg, 0.06 mmol), 1,2,4,5-tetraaminobenzene tetrahydrochloride (25.6 mg, 0.09 mmol), SDD-SiO$_2$ hard template (22.5 mg) and aluminum chloride (50 mg) were mixed in a 5 mL quartz ampule and evacuated by vacuum.[2,3] The sealed ampule was heated to 350 °C at a slow heating speed of 0.5 °C/min and then incubated at this temperature for 15 hours in the muffle furnace. During the heating process, Aza-CMP-1 formed *via* a thermal polymerization process. The resultant black solid was purified through 3 cycles of careful centrifugation and washing with de-ionized water to remove the non-templated CMP solids by taking advantage of gravity difference. The solid at the bottom of the centrifugation tube was collected and treated with 5 wt % hydrofluoric acid overnight at room temperature. After washing with methanol and ethanol for several times and drying at 70 °C under vacuum, SDD-Aza-CMP-1 was obtained as a black powder in a yield of 64%.

1.5 Preparation of SDD-Aza-CMP-2

Hexaketocyclohexane octahydrate (18.7 mg, 0.06 mmol), 3,3'-diaminobenzidine (19.3 mg, 0.09 mmol), SDD-SiO$_2$ hard template (22.5 mg) and aluminum chloride (50 mg) were mixed in a 5 mL quartz ampule, and then sealed under vacuum.[2,3] The sealed ampule was heated to 400 °C at a slow heating speed of 0.5 °C/min and then incubated at this temperature for 15 hours in the muffle furnace. During the heating process, Aza-

CMP-2 formed via a thermal polymerization process. The resultant black solid was purified through 3 cycles of careful centrifugation and washing with de-ionized water to remove the non-templated CMP solids by taking advantage of gravity difference. The solid at the bottom of the centrifugation tube was collected and treated with 5 wt % hydrofluoric acid overnight at room temperature. After washing with methanol and ethanol for several times and drying at 70 °C under vacuum, SDD-Aza-CMP-2 was obtained as a black powder in a yield of 94%.

1.6 Preparation of SDD-Aza-CMP-3

Hexaketocyclohexane octahydrate (18.7 mg, 0.06 mmol), 2,3,5,6-tetraaminobenzoquinone (15.1 mg, 0.09 mmol), SDD-SiO$_2$ hard template (22.5 mg) and aluminum chloride (50 mg) were mixed in a 5 mL quartz ampule, and then sealed under vacuum.[2,3] The sealed ampule was heated to 400 °C at a slow heating speed of 0.5 °C/min and then incubated at this temperature for 15 hours in the muffle furnace. During the heating process, Aza-CMP-3 formed via a thermal polymerization process. The resultant black solid was purified through 3 cycles of careful centrifugation and washing with de-ionized water to remove the non-templated CMP solids by taking advantage of gravity difference. The solid at the bottom of the centrifugation tube was collected and treated with 5 wt % hydrofluoric acid overnight at room temperature. After washing with methanol and ethanol for several times and drying at 70 °C under vacuum, SDD-Aza-CMP-3 was obtained as a black powder in a yield of 92%.

2. Characterizations

Scanning electron microscopy (SEM) observations were performed on a JEOL

JSM-7401F field emission scanning electron microscope. A low accelerating voltage (1 kV with a point resolution of ~1.4 nm) was used. SEM sample was prepared by dropping a drop of the sample dispersions onto a silicon wafer, followed by drying naturally for 24 hours. Before dropping the samples, the silicon wafers were cleaned in a bath of 100 mL 80% H_2SO_4, 35 mL H_2O_2 and then 20 mL Milli-Q water at room temperature. The silicon surface was then dried with compressed nitrogen gas. **Transmission electron microscopy (TEM)** studies were performed using a JEOL JEM-2100 microscope equipped with a LaB6 gun operated at 200 kV (Cs 1.0 mm, point resolution of 2.3 Å). Images were recorded using a TENGRA CCD camera (2304 × 2304 pixels with a 2:1 fiber-optical taper and an effective pixel size of 18 μm^2). TEM sample was prepared by dropping a drop of the sample dispersions onto a copper grid, followed by drying naturally for 24 hours. **Small angle X-ray scattering (SAXS)** was recorded by synchrotron radiation at beamline BL10U1, provided by the Shanghai Synchrotron Radiation Facility (SSRF), in which the third generation of synchrotron radiation light sources was employed. The experiments were carried out through the radiation of X-ray with a wavelength of $\lambda = 0.124$ nm at room temperature (25 °C). The SAXS detector was Eiger 4 M, the number of pixels in the two directions of the detector were 2070 and 2167, respectively, and the pixel size of the detector was 75 μm. The distance between the sample and the detector was between 4.5 and 27.6 m. Typical exposure time was between 0.1 and 10 s. One-dimensional SAXS profiles were obtained by circular averaging of the corresponding two-dimensional scattering patterns. **Nitrogen adsorption-desorption isotherms** were obtained at 77 K on an

Autosorb-iQA3200-4 sorption analyzer (Quantatech Co., USA) instrument. Before measurement, samples were degassed in a vacuum at 180 °C for at least six hours. Brunauer-Emmett-Teller (BET) method was utilized to calculate the specific surface area using adsorption data in a relative pressure range from 0.06 to 0.2. The pore size distributions were derived from the adsorption branches of isotherms using nonlocal density functional theory (DFT) for the micropore diameter up to 2 nm and the Barrett-Joyner-Halenda (BJH) method for the mesopore size range of 2-50 nm, respectively. **X-ray diffraction (XRD)** patterns were recorded on a D8 DaVinci X-ray powder diffractometer over the range of 5-60° (2θ). **Fourier transform infrared (FTIR) spectra** were recorded on a Spectrum 100 (Perkin Elmer, Inc., USA) spectrometer. **X-ray photoelectron spectroscopy (XPS)** was performed on a Thermo ESCALAB spectrometer using a Thermo ESCALAB instrument equipped with a monochromated Al Kα radiation (1486.6 eV). Binding energies were corrected by reference to the C 1s peak at 284.8 eV. **Gel permeation chromatography (GPC)** GPC analyses were carried out on a Shimadzu Prominence system (GPC, LC-20A, Shimadzu, Japan) with a combination of two columns (Shodex, KF-802 and 804, 300 × 8 mm) and equipped with a RID-10A differential refractive index detector at 40 °C, using THF as the eluent at a flow rate of 1 mL/min and linear polystyrene as the standard.
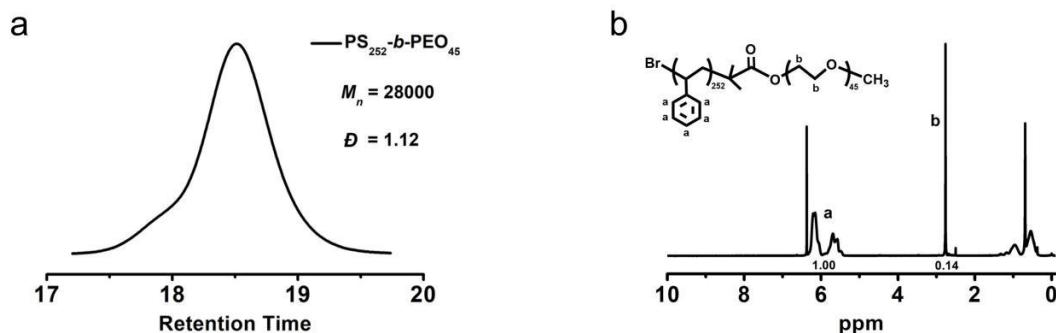
3. Characterization results of PS-*b*-PEO

Figure S2. (a) GPC trace of PS$_{252}$-*b*-PEO$_{45}$. (b) ^{1}H NMR spectrum of PS$_{252}$-*b*-PEO$_{45}$. The degree of polymerization of the PS block is calculated according to the GPC result.

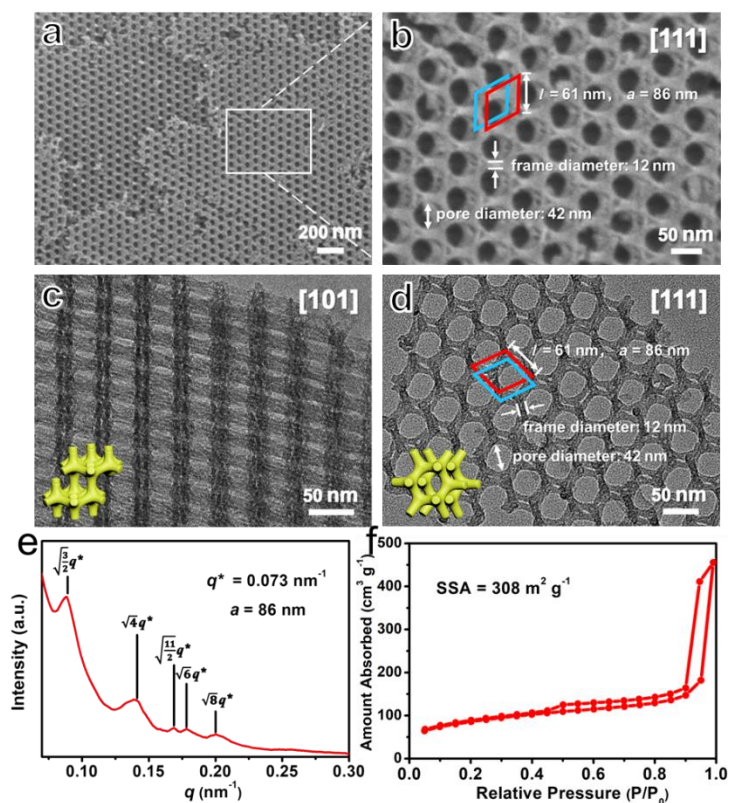## 4. Additional analysis results of SDD-SiO$_2$ and SDD-Aza-CMPs

Figure S3. Structural characterizations of dried SDD-SiO$_2$. (a) SEM image of a large area. (b) High-magnification SEM image with related sizes marked. The red and blue rhombuses stress the two shifted silica frameworks. (c,d) TEM images from different orientations with the corresponding sizes marked, the insets show the simulated models. (e) SAXS pattern, the lattice parameter $a = 2\pi/q^*$. (f) Nitrogen adsorption-desorption isotherm.
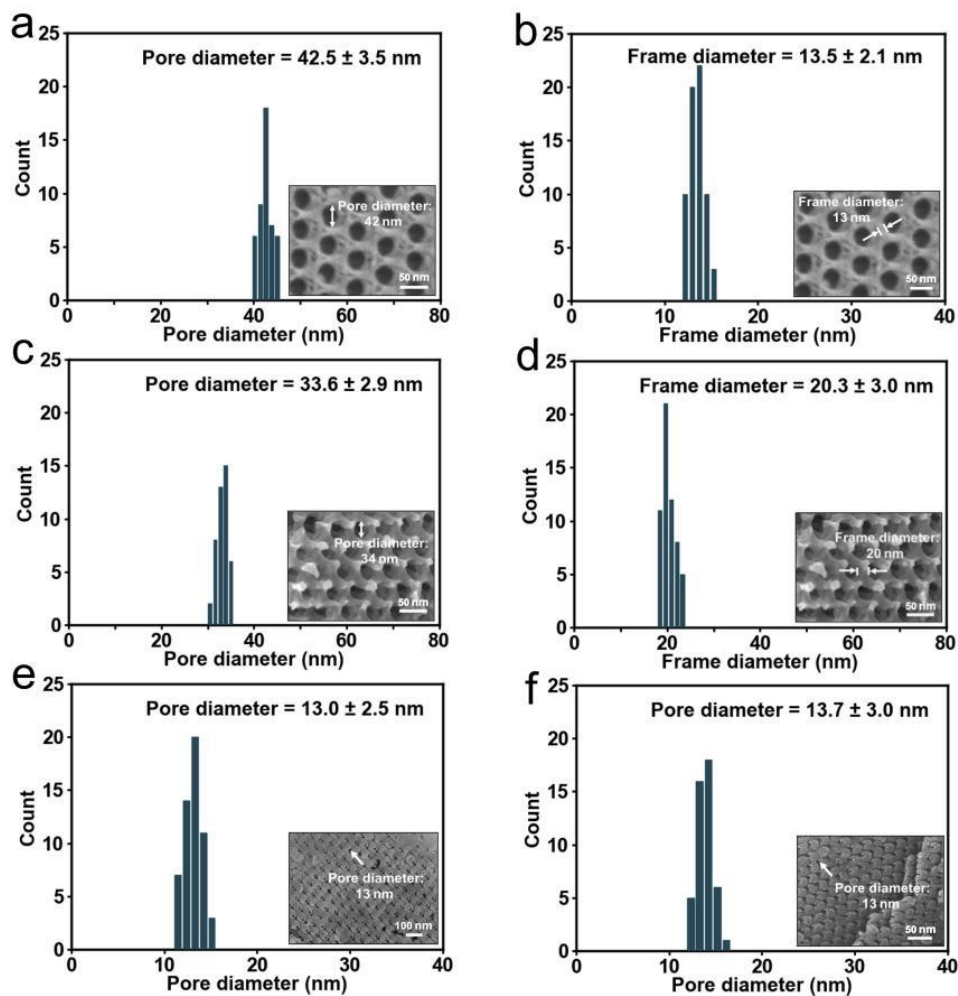
Figure S4. (a) Pore diameter distribution and the average pore diameter of SDD-SiO$_2$. (b) Frame diameter distribution and the average frame diameter of SDD-SiO$_2$. (c) Pore diameter distribution and the average pore diameter of SDD-CMP-1. (d) Frame diameter distribution and the average frame diameter of SDD-CMP-1. (e,f) Pore diameter distributions and the average pore diameters of (e) SDD-CMP-2 and (f) SDD-CMP-3. These data are based on the statistical analyses of 200 pores or frames in the corresponding SEM images.
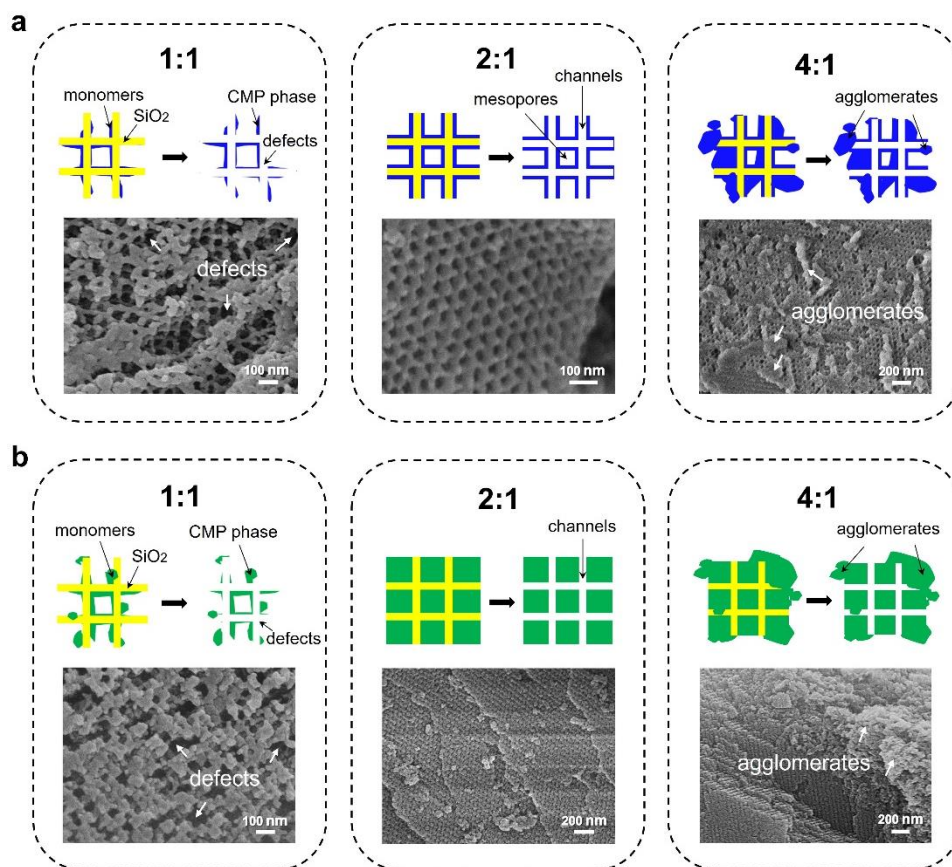
Figure S5. Schematic illustrations of the CMP morphologies obtained at different ratios of the total mass of (a) HKH and TAB to the weight of silica, along with the corresponding SEM images, and of (b) HKH and DAB (or TABQ) to the weight of silica, along with the corresponding SEM images. The 2:1 ratio is the optimal one.
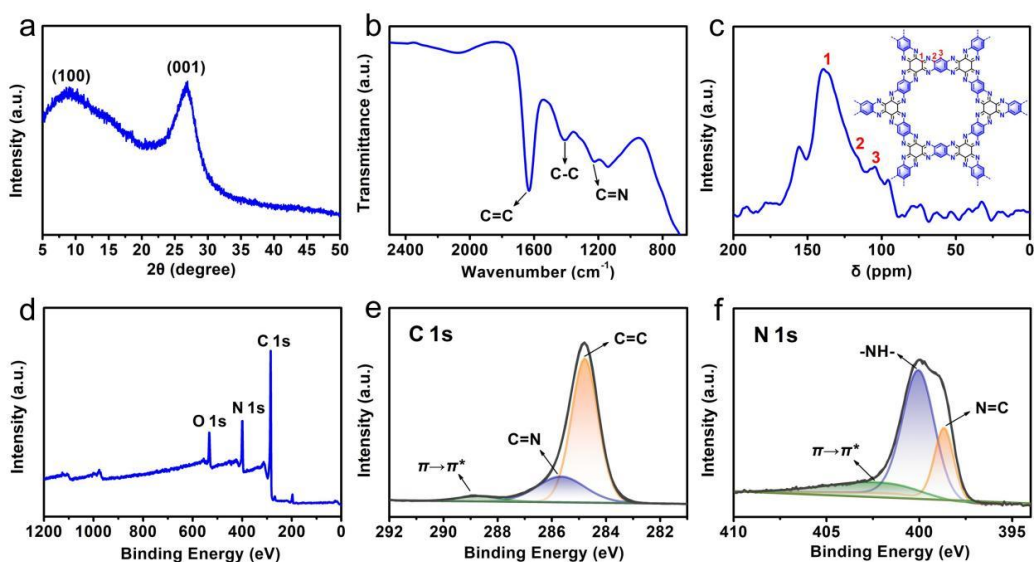

Figure S6. Characterizations of the chemical nature of SDD-Aza-CMP-1. (a) PXRD pattern. (b) FTIR spectrum. (c) Solid-state ^{13}C NMR spectrum. (d-f) XPS spectra: (d) survey; (e) C 1s; (f) N 1s.

The discussions regarding Figure S6 are given in the main text. As a supplement, in the PXRD pattern of SDD-Aza-CMP-1 (Figure S6a), the more prominent diffraction from the (001) plane compared to that from the (100) plane is probably owing to the preferential orientation along the c axis of Aza-CMP-1,[4] analogous to that of graphitic carbon nitride.[5] In the FTIR spectrum (Figure S6b), the distinct peak at 1610 cm^{-1} can be attributed to the stretching mode from the phenyl ring, originating from the TAB monomers. In addition, the signal at 1420 cm^{-1} can be assigned to the C-C stretching mode from the aromatic ring, suggesting the introduction of the cycloalkanes from the HKH monomer.[3]
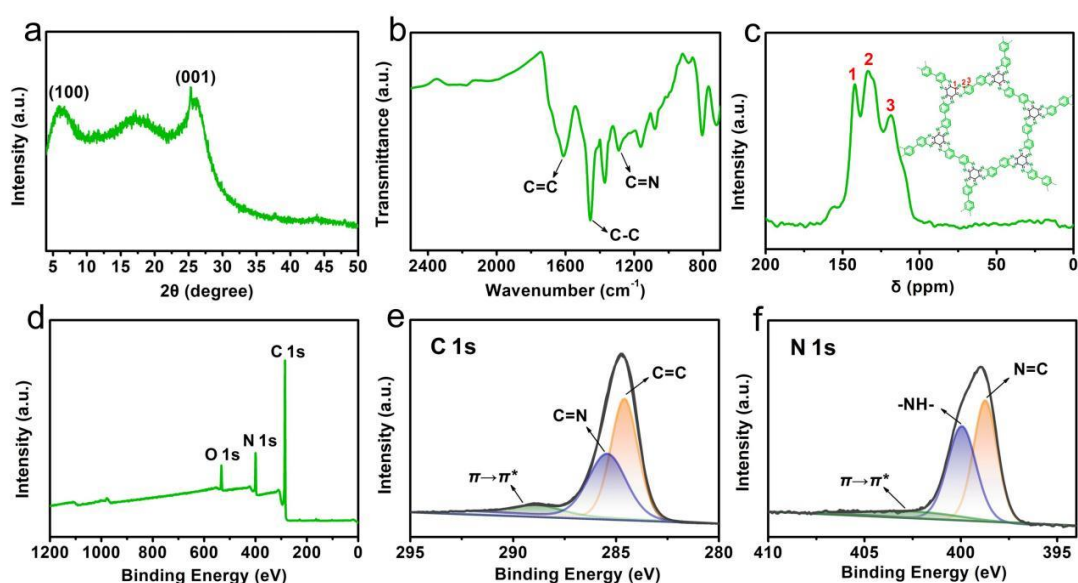

Figure S7. Characterizations of the chemical nature of SDD-Aza-CMP-2. (a) PXRD pattern. (b) FTIR spectrum. (c) Solid-state ^{13}C NMR spectrum. (d-f) XPS spectra of SDD-Aza-CMP-2: (d) survey; (e) C 1s; (f) N 1s.

The discussions regarding Figure S7 are shown in the main text. As a supplement, in the PXRD pattern of SDD-Aza-CMP-2 (Figure S7a), the signals at 2θ = 6.6° and 26.0° are attributed to the diffractions of the (100) and (001) planes, respectively. In the

FTIR spectrum (Figure S7b), the peaks at 1220 cm^{-1} and 1610 cm^{-1} indicate the formation of C=N bonds and the presence of C=C bonds of phenyl rings.[3]
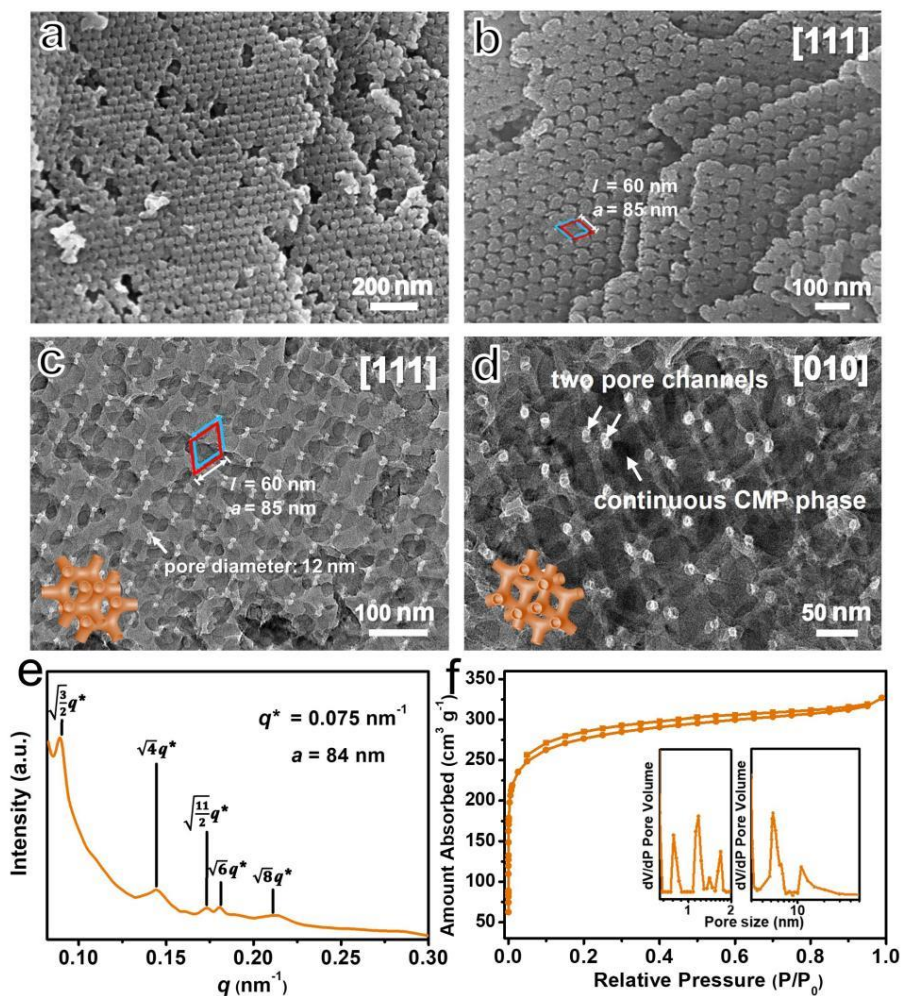

Figure S8. Structural characterizations of dried SDD-CMP-3. (a,b) SEM images. (c,d) TEM images from different orientations, the rhombuses and arrows indicate the two sets of continuous mesochannels. The insets show the corresponding calculated models. (e) SAXS pattern; the lattice parameter is calculated by $a = 2\pi/q*$. (f) Nitrogen adsorption-desorption isotherm and pore size distributions.
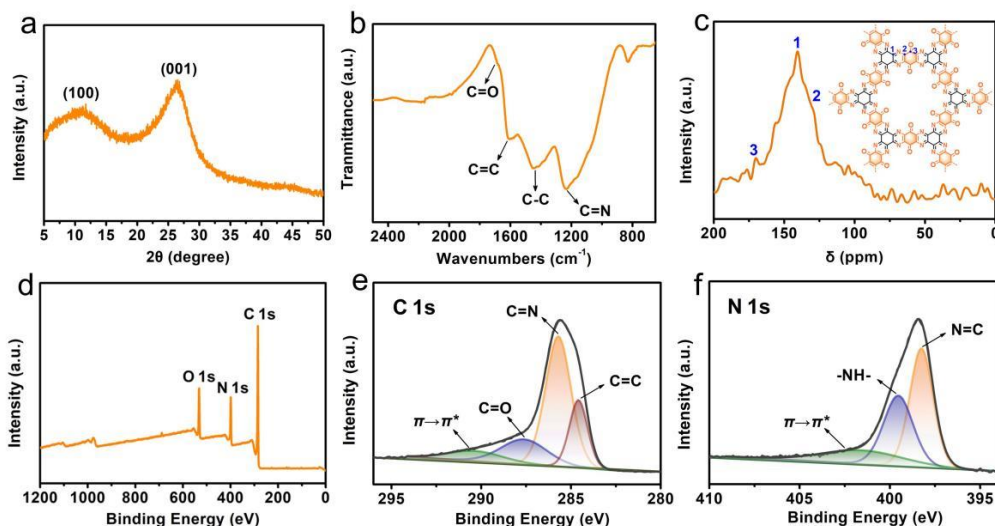
Figure S9. Characterizations of the chemical nature of SDD-Aza-CMP-3. (a) PXRD pattern. (b) FTIR spectrum. (c) solid-state ^{13}C NMR spectrum. (d-f) XPS spectra of SDD-Aza-CMP-3: (d) survey; (e) C 1s; (f) N 1s.

In Figure S9a, the PXRD pattern of SDD-Aza-CMP-3 displays several broad peaks and reveals its low crystallinity. The signal at 26.4° is attributed to the diffraction of the (001) planes, giving an interlayer distance of 0.34 nm.[6] In the FTIR spectrum (Figure S9b), the peaks at 1220 cm^{-1} and 1610 cm^{-1} indicate the formation of C=N bonds and the presence of C=C bonds phenyl rings in SDD-Aza-CMP-3, while the strong peak at 1420 cm^{-1} is attributed to C-C bonds and the peak at 1697 cm^{-1} proves the presence of C=O groups.[6] In the ^{13}C solid-state NMR spectrum (Figure S9c), the peaks at chemical shifts (δ) of 140 is assignable to the carbon atoms of C=N groups in the CMP network, proving the crosslinking of carbonyl and amino groups. The signals at 172 and 130 ppm are attributed to the carbon atoms of C=O and C=C units.[6] The C 1s XPS spectrum of SDD-Aza-CMP-3 shows the peaks at 284.6 and 285.7 eV (Figure S9e), which can be assigned to the C=C and C=N bonds, respectively. Additionally, the signal at 287.8 eV is attributed to C=O groups.[6] The N 1s spectrum confirms the presence of the N=C and -NH- units，and the π-π* characteristic peaks attributed to the

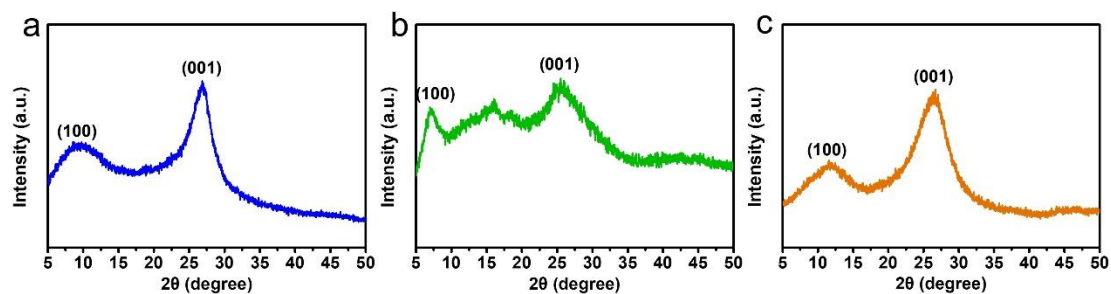π electron delocalization in the conjugated system are also observed in both of the C 1s and N 1s spectrums.[6]

Figure S10. PXRD patterns of (a) Aza-CMP-1; (b) Aza-CMP-2; (c) Aza-CMP-3. The crystallinity of the control Aza-CMP samples is highly similar to that of their corresponding SDD-Aza-CMPs (Figure S6, S7 and S9), indicating that the introduction of the bicontinuous mesostructures does not affect the crystallinity apparently.
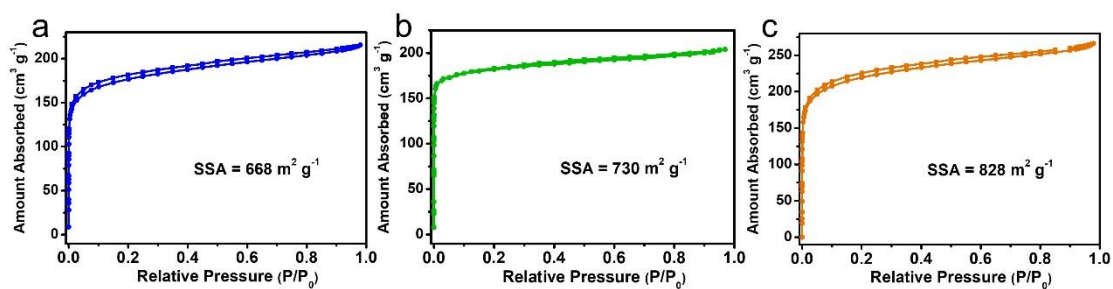

Figure S11. Nitrogen adsorption-desorption isotherms of (a) Aza-CMP-1, (b) Aza-CMP-2, and (c) Aza-CMP-3. The SSAs of the control Aza-CMP samples are a little lower than those of their corresponding SDD-Aza-CMPs, because the bicontinuous mesostructures can facilitate the N_2 gas to enter into the deep internal of SDD-Aza-CMPs, which is difficult to achieve for the control samples probably with a considerable amount of closed micropores.

5. Discussion on the formations of the different structures of SDD-Aza-CMPs

It is interesting to note that at any monomer-to-template ratios we could not obtained a reverse bicontinuous structure for SDD-Aza-CMP-1, and *vice versa*. We consider that this difference can be attributed to the different melting/boiling temperatures of the monomers for the different Aza-CMPs. To our knowledge, the HKH and TAB monomers have melting points of *ca.* 100 and 300 ºC, while their boiling points are 350 and 400 ºC, respectively.[3] Note that the boiling temperature of TAB is higher than the temperature (350 ºC) of our reaction device. After the melting of the two monomers, they could diffuse into the open mesochannels of the silica template at their liquid state and coated on the frameworks of the template. Meanwhile, at this stage the monomers might start their reaction[3] to form the polymeric layer on the frameworks as well as agglomerates adhering on the outer surfaces of the silica template. The latter situation could seal the entrance of the mesochannels and thus impeded the polymerization of more monomers inside the channels. In contrast, for SDD-Aza-CMP-2, the melting and boiling points of DAB are 176 and 250 ºC, respectively,[7] which are much lower than that of the reaction device. Before the polymerization of the monomers, probably they had evaporated and diffused into the open channels of the template at the gaseous state. At this situation, the entrances of the channels were not easy to be sealed because the probability of the aggregation formed by the gaseous monomers on the template surfaces was much lower than that from liquid monomers. Therefore, the polymerization of the gaseous monomers could continue in the silica template until the mesochannels were fully filled by the CMP phase, thus generating the reverse

bicontinuous structure for SDD-Aza-CMP-2 after the removal of the template. Similar reasons could also explain the reverse structure of SDD-Aza-CMP-3 as the TABQ monomer also has a relatively low boiling point of 290 ºC.[6]

6. Reference

1   Y. Mai, A. Eisenberg, *J. Am. Chem. Soc.*, 2010, **132**, 10081.

2   Q. Li, C. Chen, C. Li, R. Liu, S. Bi, P. Zhang, Y. Zhou, Y. Mai, *ACS Nano*, 2020, **14**, 13655.

3   Y. Kou, Y. Xu, Z. Guo, D. Jiang, *Angew. Chem. Int. Ed.,* 2011, **123**, 8913.

4   A. J. Howarth, A. W. Peters, N. A. Vermeulen, T. C. Wang, J. T. Hupp, O. K. Farha, *Chem. Mater.*, 2017, **29**, 30.

5   X. Wang, K. Maeda, A. Thomas, K. Takanabe, G. Xin, J. M. Carlsson, K. Domen, M. Antonietti, *Nat. Mater.*, 2009, **8**, 77.

6   S. Kandambeth, J. Jia, H. Wu, V. S. Kale, P. T. Parvatkar, J. Czaban-Jóźwiak, S. Zhou, X. Xu, Z. O. Ameur, E. Abou-Hamad, A. H. Emwas, *Adv. Energy Mater.*, 2020, **10**, 2001673.

7   J. Wang, C. S. Chen, Y. Zhang, *ACS Sustainable Chem. & Eng.*, 2018, **6**, 1773.